Growth and cell survival are unevenly impaired in *pixie* mutant wing discs

Carmen M. A. Coelho[1,2], Benjamin Kolevski[1], Caroline Bunn[1], Cherryl Walker[1], Anupama Dahanukar[3] and Sally J. Leevers[1,*]

[1]Cancer Research UK London Research Institute, PO Box 123, 44 Lincolns Inn Fields, London WC2A 3PX, UK
[2]National Centre for Biological Sciences, UAS-GKVK Campus, Bellary Road, Bangalore 560 065, India
[3]Department of Genetics, Howard Hughes Medical Institute, Duke University Medical Center, Durham, NC 27710, USA
*Author for correspondence (e-mail: sally.leevers@cancer.org.uk)

Accepted 4 October 2005

Development 132, 5411-5424
Published by The Company of Biologists 2005
doi:10.1242/dev.02148

Summary

It is largely unknown how growth slows and then stops in vivo. Similar to most organs, *Drosophila* imaginal discs undergo a fast, near-exponential growth phase followed by a slow growth phase before final target size is reached. We have used a genetic approach to study the role of an ABC-E protein, Pixie, in wing disc growth. *pixie* mutants, like mutants in ribosomal proteins genes (known as *Minutes*), show severe developmental delay with relatively mild alterations in final body size. Intriguingly, *pixie* mutant wing imaginal discs show complex regional and temporal defects in growth and cell survival that are compensated to result in near-normal final size. In S2 cells, Pixie, like its yeast homolog RLI1, is required for translation. However, a comparison of the growth of eukaryotic translation initiation factor *eIF4A* and *pixie* mutant clones in wing discs suggests that only a subset of translation regulators, including *pixie*, mediate regional differences in growth and cell survival in wing discs. Interestingly, some of the regional effects on *pixie* mutant clone growth are enhanced in a *Minute* background. Our results suggest that the role of Pixie is not merely to allow growth, as might be expected for a translation regulator. Instead, Pixie also behaves as a target of putative constraining signals that slow disc growth during late larval life. We propose a model in which a balance of growth inhibitors and promoters determines tissue growth rates and cell survival. An alteration in this balance slows growth before final disc size is reached.

Key words: Cell growth, Ribosomal proteins, *Drosophila*

Introduction

Despite the significant advances made in the understanding of growth control in vivo, the mechanisms that stop organ growth at a defined final size remain a mystery. In most tissues, growth slows before it stops (reviewed by Bryant and Simpson, 1984). Thus, an exponential phase of tissue growth, during which growth per unit time is proportional to the mass that already exists, is followed by a slower growth phase, during which growth per unit time is proportional to the amount of growth 'yet to come' (see Bryant and Simpson, 1984). In mammals, extensive data show that growth begins to slow at different times and slows at different rates amongst different organs (Farmer and German, 2004; Stewart and German, 1999). The ability to sense size may determine when growth begins to slow, as diet restrictions that slow growth also delay the final slowing of growth, allowing target size to be reached (Reichling and German, 2000). The developmentally regulated slow-down of growth normally occurs in the presence of ample nutrients and growth factors, and hence requires specific mechanisms that restrain growth-promoting signals. Little is known about how growth deceleration is regulated in vivo.

The *Drosophila* imaginal disc represents an ideal model system with which to study the regulation of tissue growth. Imaginal discs are epithelial sacs that develop during larval life to give rise to most of the adult structures (Cohen, 1993). Growth during larval life is the major determinant of adult size. Intrinsic mechanisms allow discs to grow to their normal final size even in the presence of ample nutrients; for example, when they are transplanted to adult hosts (Bryant and Levinson, 1985) (reviewed by Day and Lawrence, 2000). During normal disc development, disc cell number increases approximately exponentially from the end of the first larval instar until it slows around the middle of the third and final instar. Some developmental constraints on growth are likely to exist during the fast phase (Garcia-Bellido and Merriam, 1971; Gonzalez-Gaitan et al., 1994; Milan et al., 1996; Johnston and Sanders, 2003). Importantly, final organ size sensing mechanisms sense and control disc size rather than disc cell number (Neufeld et al., 1998; Day and Lawrence, 2000). Furthermore, there is no evidence for a cell size checkpoint and it is likely that growth (increase in mass) and cell division are regulated independently of each other (Neufeld et al., 1998; Leevers and Hafen, 2004; Prober and Edgar, 2000; Datar et al., 2000; Coelho and Leevers, 2000). A mild degree of cell death occurs during most of imaginal disc development (Milan et al., 1997). Recent work suggests that this cell death is necessary to maintain reproducible organ size (de la Cova et al., 2004).

There are a few hints of temporal changes in the growth

Development

Development

promoting activity of specific signalling pathways during late imaginal disc growth. For example, late in larval development, wing disc cells seem to become refractile to growth-inducing signals from a constitutively activated Dpp receptor (Martin-Castellanos and Edgar, 2002). Thus unknown factors may inhibit the ability of wing discs cells to respond to Dpp after the larval growth period. Two potential inhibitors of late disc growth have been identified. Nitric oxide (NO) inhibits imaginal disc cell proliferation, and NO levels have been shown to increase in late third instar imaginal discs (Kuzin et al., 1996). Wg signalling mediates cell-cycle arrest at the dorsoventral boundary during the third instar as part of the program of disc differentiation (Johnston and Edgar, 1998). More recent work has suggested that this role of Wg signalling in cell cycle arrest may extend to the rest of the wing pouch during the late third instar (Johnston and Sanders, 2003; Giraldez and Cohen, 2003).

Growth and cell division rates are not uniform within wing discs, and mild regional differences may contribute to the shape of these discs. Johnston and Sanders (Johnston and Sanders, 2003) report that median cell doubling times are slower in the wing pouch (which gives rise to the adult wing blade) than in the wing hinge (see Postlethwait, 1978). In addition, growth is faster in the posterior compartment, which in early discs is smaller than the anterior compartment (Garcia-Bellido and Merriam, 1971; Neufeld et al., 1998). Within the wing pouch, an evaluation of clone frequencies and their spatial distribution suggested that there might be pulses of proliferation that act within intervein regions (Gonzalez-Gaitan et al., 1994). It is not clear what determines these regional differences in growth and cell division rates. Indeed, cell division rates in early discs do not reflect the distribution of the known morphogens Wg and Dpp (Milan et al., 1996; Martin-Castellanos and Edgar, 2002). Interestingly, reducing Myc or ribosomal protein (Rp) function in wing imaginal disc clones results in region-specific effects on clonal growth. These effects have been attributed to regional differences in the severity of cell competition (Simpson, 1979; Moreno et al., 2002; Moreno and Basler, 2004).

We report here the role in growth control of Pixie, an ATP-binding-cassette (ABC) domain protein with two N-terminal iron-sulphur-binding domains. Although many ABC proteins are transporters that possess transmembrane domains, Pixie belongs to the ABC-E subfamily of ABC proteins, which, like the ABC-F subfamily, lack trans-membrane domains (Dean and Allikmets, 2001). Several ABC-E and ABC-F proteins have recently been shown to play roles in the regulation of translation (reviewed by Kerr, 2004). The yeast homolog of Pixie, RLI1, functions in translation-initiation complex formation and ribosomal biogenesis and thus may provide a functional link between assembly of iron sulphur clusters, ribosomal biogenesis and translation initiation (Kispal et al., 2005; Yarunin et al., 2005; Dong et al., 2004).

Here, we show that in *Drosophila* S2 cells, Pixie is required for translation and that *pixie* mutants behave like recessive *Minutes*. Both *pixie* and *Minute* mutant wing discs show complex defects in growth and cell survival that vary temporally and spatially. These defects are compensated such that near normal final body size and pattern are achieved. Clonal analysis in wing discs suggests that in keeping with its role as a translation regulator, *pixie* is required for growth. Interestingly during the late, slow growth phase, *pixie* mutant clones are smallest in regions of the disc where growth is slowest. Together our data are consistent with a model in which *pixie* function is a target of the growth constraining signals that slow growth during late larval life.

Materials and methods

Fly stocks

The following fly strains were generated or obtained from the Bloomington stock centre, unless otherwise indicated: *y w*; FRT80B, *y w* hs-flp^{122}; Ubi-GFP FRT80B, *y w; pix^{L17}* FRT80B/TM3 Sb Kr-GFP, *w* hs-flp^{122} *f^{36a}*; *mwh* P[f^{+64C} w^{+}] FRT80B/TM1 *mwh* (a gift from A Garcia-Bellido), *y w* hs-flp^{122}; *M(3)66D^{1}* Ubi-GFP FRT80B/TM6B *Tb*, *y w/w*; UAS-p35; *pix^{L17}* FRT80B/SM6-TM6, *y w* hsflp^{122}; En-Gal4; Ubi-GFP FRT80B/ SM6-TM6B, En-Gal4; *pix^{L35}* FRT80B / SM6-TM6B, *y w* hs-flp^{122}; Ubi-GFP FRT40A and *w; eIF4A^{1006}* 40AFRT/CyO (a gift from M Galloni) (Galloni and Edgar, 1999).

For most experiments, larvae were collected from short egg lays and reared at defined densities, in order to avoid asynchrony.

dsRNAi

dsRNAi was performed by adding 10 μg dsRNA to 35 mm wells containing 2×10^6 *Drosophila* Schneider S2 cells as described (Clemens et al., 2000). DNA templates containing 5′ T7 RNA polymerase-binding sites were PCR amplified from plasmid or genomic DNA and transcribed with the Megascript T7 transcription kit (Ambion). Primers contained 5′ T7 RNA polymerase-binding sites preceded by a GAA overhang followed by sense or antisense sequences: *pixie* sense primer, GGAGAAGCACACAACGCATCG; *pixie* antisense primer, TGATCGAATGGTCAAGGCAGC; *eIF4A* sense primer, GCATCTTGGAATCCGGTTGCC; *eIF4A* antisense primer, GTTGCAGAAGATTACCGACTGG.

Translation assays

S2 cells (8×10^6 per point) were incubated for 3 hours in 1 ml Schneider's *Drosophila* medium (Gibco), 10% foetal bovine serum, containing 200 μCi Promix [^{35}S] cell labelling mix (1000 Ci/mMol, Amersham Biosciences). For emetine treatment, cells were pre-treated for 30 minutes in 0.1 mM emetine (Sigma), prior to addition of Promix. Cells were lysed in 100 μl per point of lysis buffer [50 mM HEPES (pH 7.5), 1% Triton X-100, 150 mM NaCl, 2 mM EDTA, 2 mM EGTA, 1 mM $NaVO_4$, 50 mM NaF, 10 μg/ml aprotinin, 1 μg/ml leupeptin, 10 μg/ml Pepstatin A, 15 μM TLCK, 1 mM PMSF], and aliquots were removed for protein assay (BioRad DC protein assay kit) and analysis by western blotting. Incorporation of [^{35}S]cysteine and [^{35}S]methionine into total cellular protein was assessed by TCA precipitation. Aliquots (5 μl) of lysate were added to 0.5 ml water and 0.5 ml of 0.5 M NaOH containing 1 mM L-methionine and L-cysteine in glass tubes. Tubes were vortexed, incubated at 30°C for 10 minutes, then 1 ml cold 25% (w/v) TCA was added. Tubes were vortexed and incubated on ice for 5 minutes. Precipitated [^{35}S]-labelled proteins were collected by filtration through Whatman GFC glass fibre filters, washed three times in 5% cold TCA, rinsed in 95% ethanol, dried and quantified by scintillation counting. Each dsRNAi condition was carried out in duplicate, and [^{35}S]cysteine and methionine incorporation into protein was measured in duplicate.

Sucrose sedimentation and western blotting

S2 cells were lysed at a density of 10^8 cells per ml in SDG100 or SDG500 (high salt lysis) buffer (Tyzack et al., 2000) with 0.05 M NaF, 1 mM $NaVO_4$, 0.01% Pepstatin, 0.01% Aprotinin, 0.015 mM TLCK, 0.001% Leupeptin, 1 mM PMSF. Cleared lysates were run through 0.8 M sucrose cushions in the presence of 100 mM or 500 mM (high

Development

salt) KCl at 290,000 ***g*** in a TLA110 rotor for 2 hours. The samples were collected as described (Tyzack et al., 2000) and analyzed by western blotting. Anti-Pixie polyclonal rabbit antisera were raised against the C-terminal peptide: KDTEQKRSGQFFFLEDEACN, coupled via its N-terminal amino group and glutaraldehyde to KLH (Pierce). Anti-DAkt antiserum has been described previously (Lizcano et al., 2003). Anti-ribosomal-P antigen (ImmunoVision) was used at 1:200. Western blots were probed with secondary antibodies labelled with Alexa Fluor 680 (Molecular Probes) or IRDye800 (Rockland Immunochemicals) and scanned using the Odyssey Infrared Imaging System (LI-COR Biosciences).

Mitotic recombination and clonal analysis

Mitotic recombination was induced using the FLP/FRT system (Xu and Rubin, 1993). Wild-type or pix^{L17} clones were generated by heat-shocking *y w*; FRT80B/Ubi-GFP FRT80B or *y w*; pix^{L17} FRT80B/Ubi-GFP FRT80B larvae at 34°C for 30 minutes (clones induced during second instar) or 15 minutes (clones induced during third instar). Similar methods were used to generate $eIF4A^{1006}$ clones. To examine clones in adult wings, *w* hs-flp^{122} f^{36a}; pix^{L17} FRT80B/*mwh* P[f^{+64C} w^{+}] FRT80B larvae were heat-shocked for 45-80 minutes and male wings were examined.

Clone median doubling time (MDT) was calculated by dividing the number of hours of the clone induction window by $\log_2$ (Median clone cell number). As is shown in Fig. 6A, the early clone induction windows overlap by 5 hours with the late 32-hour window, and by 17 hours with the late 44-hour window. Despite this difference in the period of overlap with a faster growth phase, the twin MDT within the two late windows is similar. By contrast, twins generated using the 60 hour clone induction window have a MDT that is intermediate between the fast and slow phases. Because of the lag time between heat-shock and clone generation, the actual overlap of the 32, 37 and 44 hour late windows with the fast phase is likely to be minimal, whereas the 60 hour window spans both fast and slow growth phases (Fig. 6A,D; an intermediate MDT is also observed with other short windows that span the fast and slow phases, data not shown). X-ray induced mitotic clonal analyses revealed exponential growth, with decreases in rate at the larval moults (average MDT=8.5 hours) (Garcia-Bellido and Merriam, 1971). However Johnston and Sanders suggest that MDT increases gradually as development progresses (in the hinge it is 9.5 hours during early second instar to 11.5 hours in the third instar) (Johnston and Sanders, 2003). Our data reveal a fast growth phase followed closely by a slower growth phase, approximating the growth curve demonstrated by Byrant and Levinson (Byrant and Levinson, 1985). Owing to the limitations of the clonal analysis technique, our data do not suggest the rate of deceleration of cell division during late third instar.

To generate clones in a *Minute* background, *y w*; FRT80B or *y w;* pix^{L17} FRT80B/TM3 Sb, Kr-GFP males were mated with *y w* hs-flp^{122}; $M(3)66D^{1}$ Ubi-GFP FRT80B/TM6B *Tb* females and larvae were heat-shocked for 10 minutes. Tb^{+} larvae were dissected. Poor-growing mutant clones are often observed as fragments around a wild-type twin clone. When clones have a growth advantage over their surrounding tissue, they generally do not fragment, allowing easy recognition of clone boundaries. In the late hinge in the *Minute* background, there is a high frequency of smaller pix^{L17} clones, which contribute to an estimated decrease in hinge MDT when compared with the MDT of these clones in a $Minute^{+}$ background. In these experiments in a *Minute* background, $Minute^{-/-}$ twins survive poorly during the late clone induction windows. In the absence of any associated twins, clone fragments belonging to the same mutant clone may be counted as separate smaller clones. Thus, the estimated MDT is likely to be lower than the actual MDT. In the pouch in a *Minute* background, pix^{L17} clone size and frequency is low, allowing us to be confident of their poor growth when compared with a $Minute^{+}$ background.

Histology

Larvae were dissected in PBS and discs fixed in 4% formaldehyde (EM grade, Polysciences) in 0.1 M PO_4 buffer (pH 7.2) for 40 minutes. S2 cells were seeded on dishes containing coverslips (MaTek), pre-coated with poly-L-lysine (Sigma), then fixed in 4% formaldehyde in 0.1 M PO_4 buffer, pH 7.2 for 20 minutes and permeabilized in 1% TritonX-100 in PBS for 3 minutes. Nuclei were labelled with 10 μg/ml propidium iodide (PI) or To-PRO-3 (Molecular Probes) at 1:2000 after RNaseA treatment (200 μg/ml; Sigma). Rhodamine-conjugated phalloidin was used at 1:60. Anti-En monoclonal 4d9 (Developmental Hybridoma Bank, Irvine, USA) was used overnight at 1:1000 as described (Brower, 1986) and anti-Pixie polyclonal antisera (see above) was used overnight at 1:5000 in PBS with 0.1% Tween 20 (PBST) with 5% normal goat serum (Vector Laboratories). Secondary antibodies used were Alexa Flour 546-coupled anti-mouse IgG (Molecular Probes) and Alexa Flour 488-coupled anti-rabbit IgG (Molecular Probes) both at 1:500 in PBST. Discs were mounted in Vectashield (Vector Labs). Apoptosis was detected using Apoptag Red (Intergen) reagents as described (White et al., 2001).

Growth curve of wing discs

Larvae were picked on hatching from 2-hour egg lays and seeded at 40 larvae per standard fly tube and maintained moist at 25°C. Approximately ten larvae were dissected per tube at various time intervals after egg lay (AEL). As there is an inherent variability in *Minute* disc size evident even at the end of larval life, discs from the larger 20% of the larvae were selected for analysis. To count the number of cells per disc, discs of early stages (before the disc folds were deep) were fixed and stained with PI as above. Confocal images were collected 2.5 μm apart in a *z*-series using a C-Apochromat 40×/1.2 W corrected lens. Cells were counted within 500 μm squares and the average number per square was determined. The area of discs was estimated using the LSM image browser (Zeiss software) and used to calculate total cell number. Older discs were dissociated in 25 to 45 μl Trypsin-EDTA in PBS for 3 to 5 hours at 37°C. Disc cell suspensions were made by repeated pipetting then 10 μl was loaded onto a haemocytometer and the cells were counted. Discs from the same larva (CS larvae, ~110 hours AEL) were counted using both techniques and the average difference in result was ~5%.

Microscopy

Confocal images were collected using a Zeiss LSM 510 confocal microscope and C-Apochromat 40×/1.2 W corrected and Plan-Apochromat 20×/0.75 lenses (wing discs) and a 63×/1.2 W corrected lens (S2 cells). Wing area, wing circumference and thorax circumference were measured using either Photoshop or the LSM image browser software. Wings were mounted in Euparal or Canada Balsam, thoraces were mounted in agar blocks (dorsal side up) and images were generated using a Nikon Eclipse E800 microscope.

Results

Identification of *pixie*, a novel growth regulator

Mutations in *pixie* were identified in a genetic screen for dominant enhancers of a small-wing phenotype, obtained by expressing a kinase-dead version of *Drosophila* PI3-kinase (KD-Dp110, Fig. 1A-E) (Leevers et al., 1996; Coelho et al., 2005). Additional *pixie* alleles were obtained in a screen for mutations that are lethal in combination with a deficiency that uncovers *pixie* (Dahanukar et al., 1999). Subsequent genetic analyses showed that the mutations obtained in the enhancer of KD-Dp110 screen were dominant-negative alleles (Table 1). Strong *pixie* mutants are homozygous lethal, while weaker hypomorphs are viable but grow slowly, with larval periods up

Table 1. Phenotypic traits of various pixie allelic combinations

Genotype	Viability	Developmental time	Body size	Wing area (mm^2)	Bristle size
yw	Viable	10 days	Normal	1.47±0.05 (n=6)	Normal
yw; pix^{3c2}/+	Viable	10 to 12 days	Reduced	1.37±0.06 (n=7, P<0.0005*)	Reduced
yw; Df(3L)Scf-R11/+	Viable	10 days	Normal	1.49±0.05 (n=7)	Normal
yw; pix^{L35}/+	Viable	10 days	Normal	1.5±0.05 (n=12, P>0.12†)	Normal
yw; pix^{L17}/+	Viable	10 days	Normal	1.57±0.03 (n=7, P<0.005†)	Normal
yw; pix^{L24}/+	Viable	10 days	Normal	ND	Normal
yw; pix^{3c2}	Embryonic lethal	–	–	–	–
yw; pix^{L17}	Embryonic lethal	–	–	–	–
yw; pix^{L24}	Larval lethal	–	–	–	–
yw; pix^{L35}	Viable	10 days	Normal	1.45±0.04 (n=6, P>0.15†)	
yw; pix^{L35}/pix^{L24}	Viable	12 to 13.5 days	Reduced	1.38±0.08 (n=11, P<0.0005*)	Reduced
yw; pix^{L35}/pix^{L17}	Viable	12 to 15 days	Reduced	1.37±0.08 (n=9, P<0.0005*)	Reduced

yw control and heterozygotes are above, homozygotes and transallelic combinations below. Among the heterozygotes, pix^{3c2}/+ shows developmental delay and reduced wing area and body size (noted by weighing flies in batches of 10 to 20). pix^{L35} is a weak allele and homozygotes show no significant difference in wing area compared with *yw* controls. pix^{L17} and pix^{L24} are strong alleles and the transallelic combinations of pix^{L35}/pix^{L24} and pix^{L35}/pix^{L17} show significant but mild decreases in wing area compared with pix^{L35} heterozygotes (see text).

*When compared with area of *yw; pix^{L35}/+* wings.

†When compared with area of *yw* wings.

to double those of wild-type larvae (Table 1). They show mild variation from the normal body size, depending on culture conditions. This variation ranges from a ~10% decrease to a 5-10% increase (Table 1, data not shown) (Coelho et al., 2005). In addition, viable adults display slender and short thoracic macrochaetae (bristles) and occasional eye roughening (Fig. 1F-G, Table 1; data not shown). No additional effects on overall pattern or differentiation are seen. The strong developmental delay, mild variation in body size and presence of slender bristles in *pixie* hypomorphs strongly resemble the dominant phenotypes of *Minutes*, many of which encode ribosomal proteins (see Table 1) (Lambertsson, 1998). Thus, *pixie* behaves as a recessive *Minute*. By contrast, mutants in the insulin-signalling pathway, which includes Dp110, show developmental delay and have correspondingly strong decreases in body size (Leevers and Hafen, 2004).

Intriguingly, we observe disproportionate effects on the size of the different parts of the body in *pixie* mutant flies. This disproportion tends towards an increase in wing size relative to body size, represented by an increase in ratio of wing circumference to thorax circumference, when compared with control (P<0.0000005, Fig. 1L). Similar, but slight variations in wing size relative to thorax size were observed in an *RpL14* mutant, $M66D^1$ (P=0.0008, Fig. 1L).

pixie encodes an ABC-E protein required for translation

Genetic mapping revealed that *pixie* encodes an ABC-E protein that possesses two N-terminal iron-sulphur binding domains and two C-terminal ABC domains (Coelho et al., 2005) (see Introduction and Fig. 2A,B). DNA sequence analysis of *pixie* alleles identified mis-sense mutations in conserved residues in both the ABC and iron-sulphur domains, confirming that both are essential for Pixie function (Fig. 2B and legend). Diverse cellular functions have been assigned to the human homolog of Pixie, RLI, including inhibiting RNaseL, aiding lentivirus capsid assembly and stabilizing MyoD mRNA (Kerr, 2004; Zimmerman et al., 2002; Dooher and Lingappa, 2004; Bisbal et al., 2000). Given that the yeast homolog of Pixie is involved in ribosomal biogenesis and translation initiation (Kispal et al., 2005; Yarunin et al., 2005; Dong et al., 2004), and the phenotypic similarities between *pixie* and the *Minutes*, we investigated whether Pixie is also involved in translation. Immunostaining revealed that Pixie is predominantly cytoplasmic in *Drosophila* S2 Schneider cells and imaginal discs (see Fig. S1 in the supplementary material and Fig. 3), consistent with a role in translation. dsRNAi-mediated depletion of Pixie from *Drosophila* S2 cells significantly lowers global translation within 2 days (Fig. 2C). Furthermore, sucrose sedimentation experiments suggest that Pixie associates with ribosomes in a salt-sensitive manner, suggesting that the association is peripheral and Pixie is not a part of the core ribosomal complex (Fig. 2D). Further biochemical analyses also suggest that Pixie, like yeast RLI1, is required for normal translation (D. Andersen and S.J.L., unpublished).

pixie hypomorph wing discs display distinct patterns of elevated cell death

pixie hypomorphs are developmentally delayed and have extended larval periods during which the growth of both whole larvae and imaginal discs is slowed. A higher than normal level of apoptosis is observed in *pixie* mutant wing discs (compare Fig. 4B with A, Fig. 4F-G with C). This increased apoptosis changes from uniformly distributed clusters during the early to mid third-instar (Fig. 4B) to a distinct pattern in the late third instar. In these late third instar discs (9/12 discs examined a day before wandering and 5/16 examined at wandering), the apoptosis is particularly intense in the wing pouch (Fig. 4F) and there is consistently less apoptosis in the hinge than elsewhere in the disc. Shortly before pupation (in the remaining discs examined a day before and at wandering) apoptosis is less intense and more uniformly distributed (Fig. 4G). Nevertheless, at this stage, it is often elevated at the dorsoventral (DV) boundary and at the edges of the pouch (thin and thick arrow in Fig. 4G). Thus, there is a transient period during late third instar well before pupation, when apoptosis is intense in the wing pouch. Interestingly, the wing discs of two *Minutes*, $M(3)66D^1$/+ and $M(3)95A^1$/+ also show a similar pattern of apoptosis during early to mid-third instar

Development

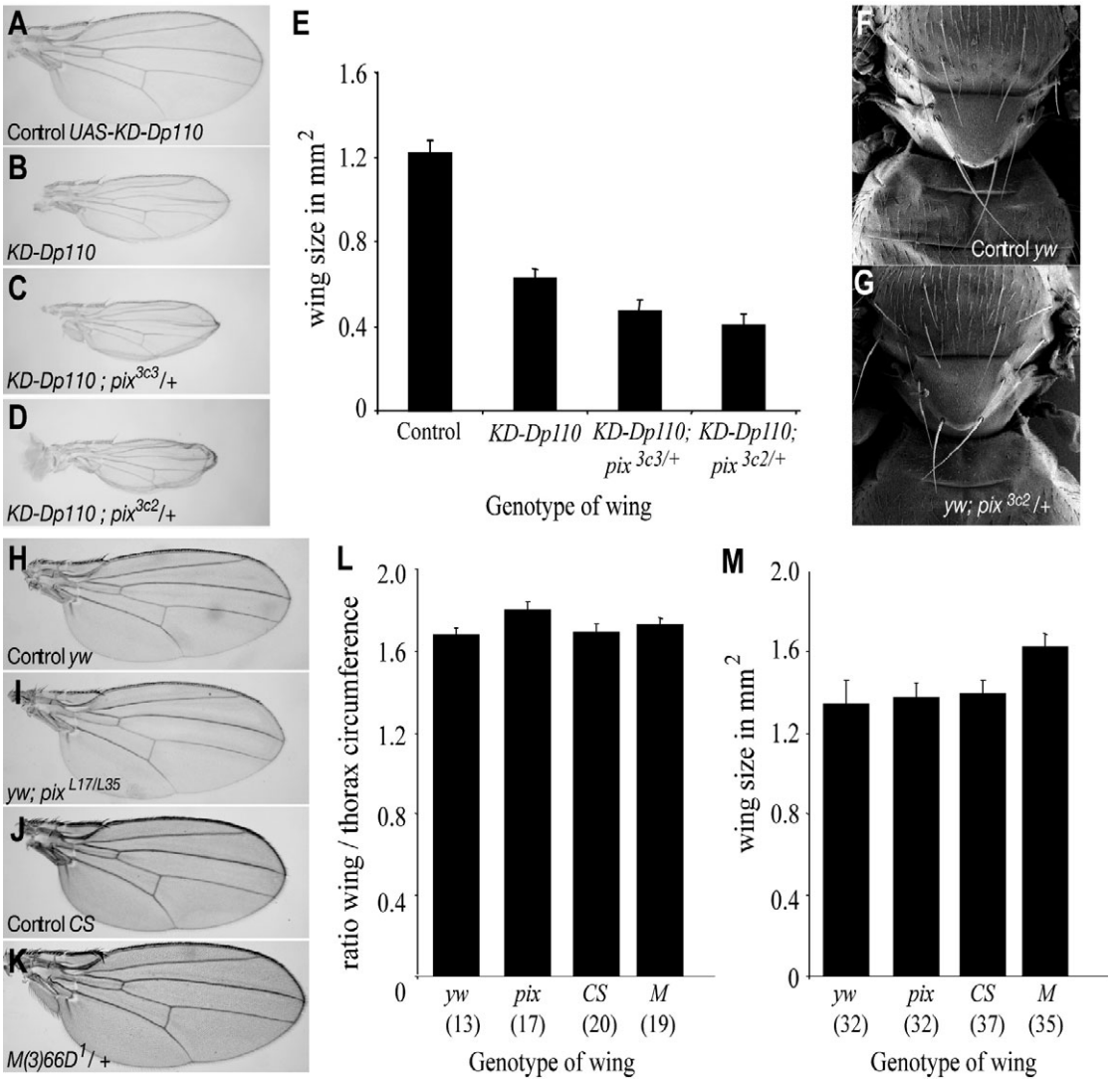

Fig. 1. *pixie* is an enhancer of a KD-Dp110-induced small-wing phenotype and shows *Minute*-like characteristics. (A--D) MS1096-Gal4 driven expression of UAS-KD-Dp110 reduces wing size and this phenotype is enhanced by pix^{3c2}/+ and pix^{3c3}/+. The genotype *MS1096>KD-Dp110* is abbreviated to *KD-Dp110*. (E) Bar chart showing the average areas of the wings in A-D, *n*=8-12. (F,G) pix^{3c2}/+ bristles (G) are shorter and more slender than control (F). (H-K) *pixie* mutant and *M(3)66D*/+ wings. Patterning defects are absent. Controls match the genetic background of the mutations, CS, CantonS. (L,M) Bar charts showing average ratio of wing/thorax circumference (L) and wing area (M) for the genotypes in H-K, *n* indicates numbers of flies/wings analyzed. When compared with control, the ratio in L is higher in $pix^{L17/L35}$ (*pix*) flies and $M66D^{1}$/+ (*M*) flies (P=3.4×10^{-10} and 0.0008, respectively). *pixie* mutant wing area is not significantly different from control, whereas $M66D^{1}$/+ wings are significantly larger than control (P=0.15 and 3.7×10^{-25}, respectively).

(see Fig. S2 in the supplementary material and data not shown) and late third instar (Fig. 4H,I,K).

Immunostaining revealed that Pixie is expressed uniformly in early and late third instar wing discs (Fig. 3). Thus, the regional differences in cell death in *pixie* mutant discs are unlikely to reflect differing expression levels of the protein in wild-type discs. The adult wings that these discs give rise to, are patterned normally, making it unlikely that the elevated cell death is due to defects in patterning or differentiation (Fig. 1H-K). Furthermore, expression of Vg, a target of Wg signalling is normal in *pixie* mutant and *Minute* discs (data not shown).

Although cell death is elevated in the wing discs of *pixie* hypomorphs, the resulting adults have a near normal body size, suggesting that extra cell divisions must compensate for the increased cell death. Indeed, the unusual increase in *pixie* hypomorph wing size relative to thorax size may be partly due to such compensatory cell division. Expression of the Caspase inhibitor, p35, in the posterior compartment of *pixie* mutant discs increases the ratio of posterior compartment size to anterior compartment size, relative to that in control wings also expressing p35 in the posterior compartment (Fig. 4M-N) (Hay et al., 1994). It has recently been shown that induction of the cell death pathway can generate a growth-promoting signal that increases wing size, when the execution of cell death itself is suppressed by p35. Such a mechanism causes extensive overgrowth in wings in which the death inducer Hid is co-expressed with p35 and involves the expression of Wg in cells in which the death signal is activated (Huh et al., 2004; Perez-Garijo et al., 2004). We do observe that, when p35 is expressed in the posterior compartment of *pixie* mutant discs, Wg is ectopically expressed in that compartment (arrow in Fig. 4N), suggesting that a reported mechanism can operate by which the cell death might be compensated (Huh et al., 2004; Perez-Garijo et al., 2004).

pixie is required for balanced growth and cell survival in wing discs

Although mild reductions in *pixie* function can allow an

increase in cell proliferation (to compensate for cell death), stronger reductions in *pixie* function clearly reduce growth and cell proliferation. When Pixie levels are reduced through RNAi in S2 cells, cell number is reduced and an increased proportion of cells accumulate in G1, indicating that Pixie may be required for G1 to S progression (Fig. 2D, lower panels). Furthermore, wing disc clones of pix^{L17}, a strong hypomorphic lethal allele, are reduced in frequency and clone size compared with their wild-type sister clones (twins, Figs 5, 6). Inhibition of apoptosis in the posterior compartment by expression of p35 significantly rescues the frequency of pix^{L17} mutant clones (Fig. 5B-D). However, these mutant clones are still smaller than their sister clones, suggesting that *pixie* is required in the wing disc for cell division and growth as well as cell survival. When pix^{L17} mutant clones were generated late in larval life, rare clones survived to the adult wing and displayed a strong reduction in cell number but not cell size (see Fig. 5A and its legend). Together, these observations demonstrate that strong

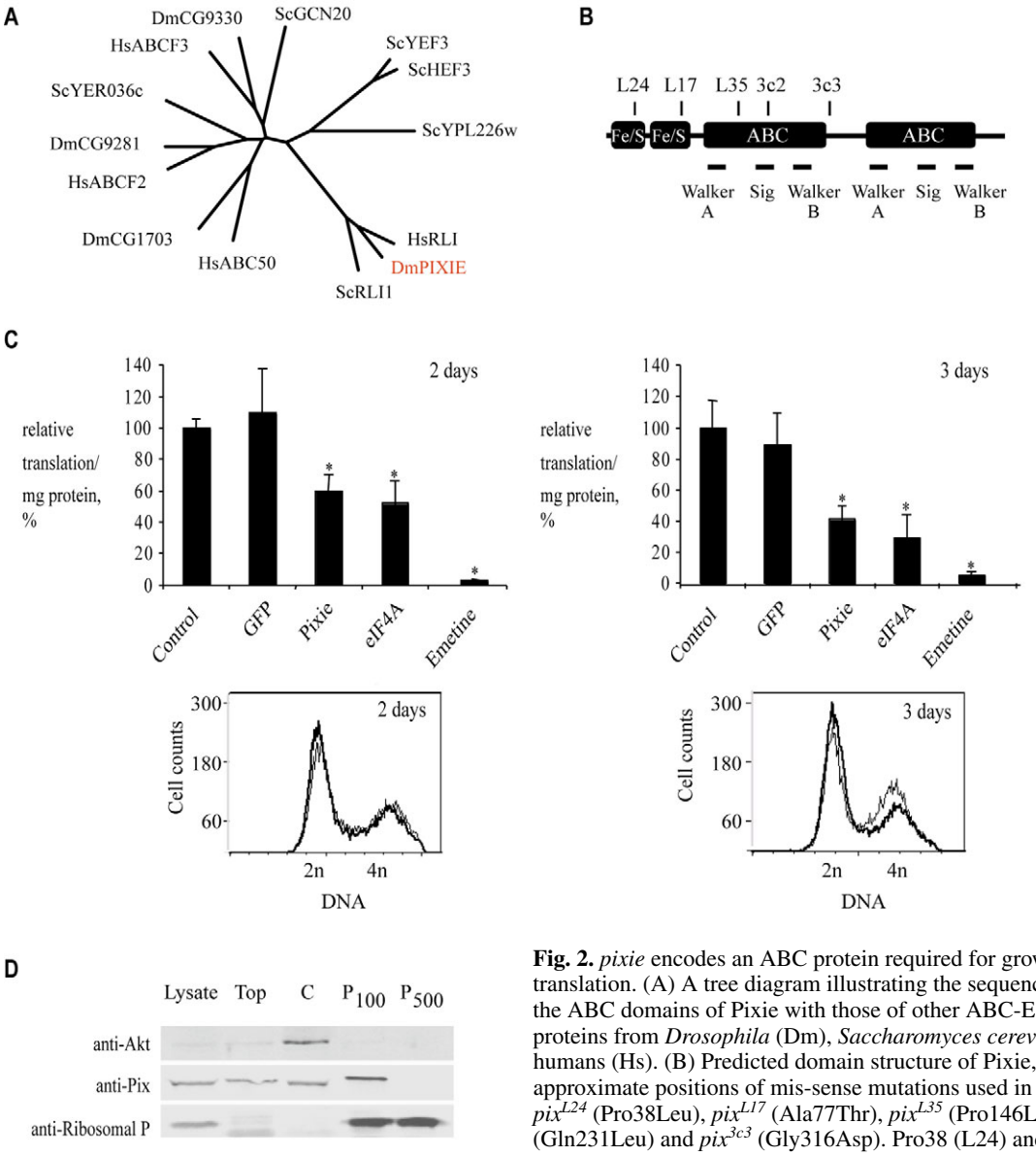

Fig. 2. *pixie* encodes an ABC protein required for growth and translation. (A) A tree diagram illustrating the sequence similarity of the ABC domains of Pixie with those of other ABC-E and ABC-F proteins from *Drosophila* (Dm), *Saccharomyces cerevisiae* (Sc) and humans (Hs). (B) Predicted domain structure of Pixie, showing approximate positions of mis-sense mutations used in this study: pix^{L24} (Pro38Leu), pix^{L17} (Ala77Thr), pix^{L35} (Pro146Leu), pix^{3c2} (Gln231Leu) and pix^{3c3} (Gly316Asp). Pro38 (L24) and Ala77 (L17) are highly conserved consensus residues of the iron-sulphur binding domains. (C) Graphs show the impact of various dsRNAi treatments on global translation, measured as [^{35}S]cysteine and methionine incorporation into total cellular protein, and represent combined data from three independent experiments. Relative translation/mg protein is expressed as a percentage of the control. In unpaired Student's *t*-tests, control and GFP do not differ; Pixie, eIF4A and emetine are significantly lower than control, **P*<0.0001. Depletion of Pixie and the translation initiation factor eIF4A was confirmed by western blotting and immunofluorescence (see Fig. S1 in the supplementary material; data not shown). Depletion of eIF4A or Pixie reduced translation by day 2, before any effect on cell number (data not shown) or cell cycle profile. Lower panels show cell cycle profiles of *pixie* RNAi-treated (thick line) and GFP RNAi control (thin line) cells obtained through FACS analysis for one of the above experiments. By day three, *pixie* RNAi treatment increases the G1 population. (D) Western blots of various fractions of an 0.8 M sucrose cushion through which S2 cells lysates were spun. Lysate, nuclei-free lysate; top, fraction above the cushion; C, cushion; P_{100}, pellet obtained in presence of 100 mM KCl; P_{500}, pellet obtained in presence of 500 mM KCl. Akt is not detected in the ribosomal pellet, whereas Pixie is (but not in the presence of high salt levels).

reductions in *pixie* function reduce both balanced growth and cell survival. Balanced growth is the term used to describe an affect on growth (increase in mass) that is accompanied by a corresponding effect on cell division, thus leaving cell size unaltered (de la Cova et al., 2004).

Changes in the regional requirement for *pixie* in clonal growth correlate with changes in disc growth rates

During our analysis of pix^{L17} mutant clones, we noticed that clones generated during late disc growth are more poorly represented in the pouch than the hinge (Fig. 5B-D, Fig. 6 and see below). This regional difference in pix^{L17} mutant clone growth persisted in the presence of p35 (Fig. 5D) and was observed with other lethal *pixie* alleles (data not shown). Like the varying pattern of cell death in hypomorphic *pixie* mutant discs (see above), the impaired growth of *pixie* mutant clones also varied with developmental stage. Closer examination of the growth curves and patterns of apoptosis in wing discs from $M(3)66D^{1}$/+larvae (which have a more uniform developmental delay than *pixie* mutant larvae) revealed that their intense cell death correlates maximally with the slow phase of growth (see Fig. S2 in the supplementary material). We thus investigated whether the strong requirement for *pixie* in pouch clone growth in late discs also correlated with the slow phase of disc growth. Although *pixie* is required for cell viability and balanced growth, we shall refer for convenience to reduced clone size and frequency in the following sections as reduced growth.

Direct cell counting methods showed that increase in cell number slows from early-mid third instar onwards (Bryant and Levinson, 1985) (see Fig. S2 in the supplementary material). Johnston and Sanders (Johnston and Sanders, 2003) have shown that wing pouch cells have a longer median doubling time (MDT) than hinge cells. The growth of the twins of *pixie* mutant clones generated in a *pix*/+ background is similar to the growth of wild-type clones generated in a wild-type background (compare Fig. 6A,D with Fig. S3 in the supplementary material), enabling an estimation of disc growth rates in our experiments. Early and late clone induction windows were chosen that allowed a similar median number of twin cell divisions (see Fig. 6D). Thus, average mutant clone/twin size is comparable between the early 29-hour and 30-hour windows and the late 44-hour and 37-hour windows (see red numbers in Fig. 6D,G). To analyze an early fast growth phase, clones were examined at the mid-third instar (pink boxes Fig. 6A,D), and to examine the late slow growth phase, clones were examined at larval wandering – the end of the larval growth period (blue boxes Fig. 6A,D). In the experiments in Fig. 6D-F, the average twin MDT during the early fast growth phase is 9.4 hours. During the late slow growth phase, the average twin MDT is 12.8 hours, 27% longer than during the fast growth phase. MDT is on average 13% longer in the pouch than the hinge, during the fast phase and 12% longer during the slow phase (see Fig. 6B,C for regional demarcation). Thus, the pouch and hinge growth rates decrease to a similar extent in going from the fast to slow phase (26 and 28%, respectively; see Materials and methods). Although not quantified, clone sizes in the presumptive thorax (notum) appear similar to those in the hinge.

During the fast growth phase (Fig. 6E) pix^{L17} mutant clone size and frequency are greatly reduced even within 29 or 30 hours of clone induction, and clones are completely absent within 46 hours. pix^{L17} clone growth is poorer in the hinge than the pouch. This is consistent with Pixie being required for translation and the fact that the hinge grows faster than the pouch, resulting in stronger competitive pressure on hinge mutant clones (see below). As disc growth slows, pix^{L17} mutant clones grow better in the hinge than during the fast phase (compare hinge data in Fig. 6E with F). Increasing the length of the clone induction window can normally strengthen the phenotype by decreasing the level of perdurant wild-type Pixie; the late windows (44 hours and 37 hours) are longer than the early windows (30 hours and 29 hours). Therefore, the better growth of *pixie* mutant clones during the late windows does reflect a lower requirement for *pixie* in the hinge during slower growth.

By contrast, pix^{L17} mutant clone growth in the pouch remains poor during part of the slow growth phase (Fig. 6F). This is most clearly seen in the 44-hour window (Fig. 6F). The sudden increase in strength of phenotype as the clone induction window is extended from 37 to 44 hours, suggests that *pixie* is strongly required in the pouch at the beginning of the slow phase. This strong requirement in the wing pouch for *pixie* at this stage was seen in two additional independent experiments (the 46 hour late window in Fig. 5D, left panels; and an additional 44 hour late window, data not shown). Furthermore, other strong *pixie* alleles have a similarly severe clone phenotype in the pouch, compared with the hinge during part of the slow growth phase (data not shown), indicating that this phenotype is not allele specific. Although not quantified, the growth of *pixie* mutant clones in the notum appears similar to that in the hinge. Thus, the growth defect of *pixie* mutant clones is unexpectedly stronger in the slower-proliferating pouch area

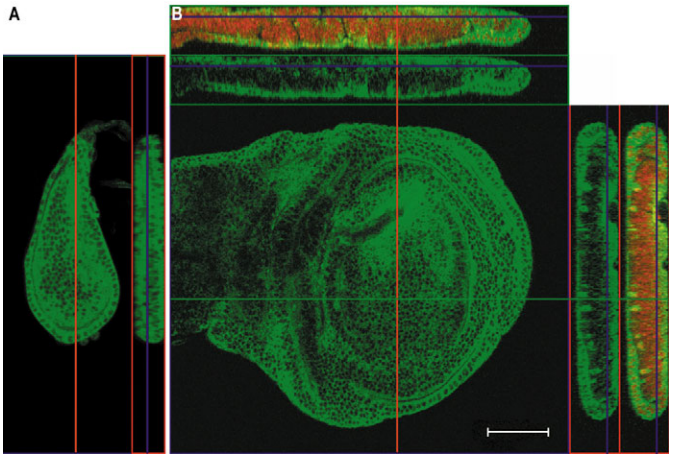

Fig. 3. Pixie is cytoplasmically localized and expressed uniformly in wing discs throughout development. Confocal images of wing discs immunostained with antiserum against Pixie. *z* sections are shown with *x*- and *y*-axis sections above and on the right respectively. The red line indicates the position of the *y*-section and the green line indicates the position of *x*-section. The blue line in the *x*- and *y*-sections depicts the position of the *z*-section. (A) Early third instar wing disc. (B) Wandering third instar disc. Additional panels above and on the right show in addition, propidium iodide staining (red), indicating the presence of nuclei in regions of the disc where Pixie staining is not detectable. Scale bar: 50 μm.

in late larval discs. Interestingly, clones that are mutant for the eukaryotic translation initiation factor, *eIF4A* show no such regional differences in their ability to grow within the wing disc during both the fast and slow growth phases (Fig. 6G).

Our results reveal a temporal and regional correlation between the growth and survival of strong *pixie* mutant clones and the pattern of cell death in hypomorphic *pixie* discs. We detect an interesting change in the regional requirement for Pixie as disc growth rates change. During the fast phase, the reduction in *pixie* mutant clone growth is stronger in the hinge and during the slow phase it is stronger in the pouch. Importantly, our clonal analysis demonstrates that during the

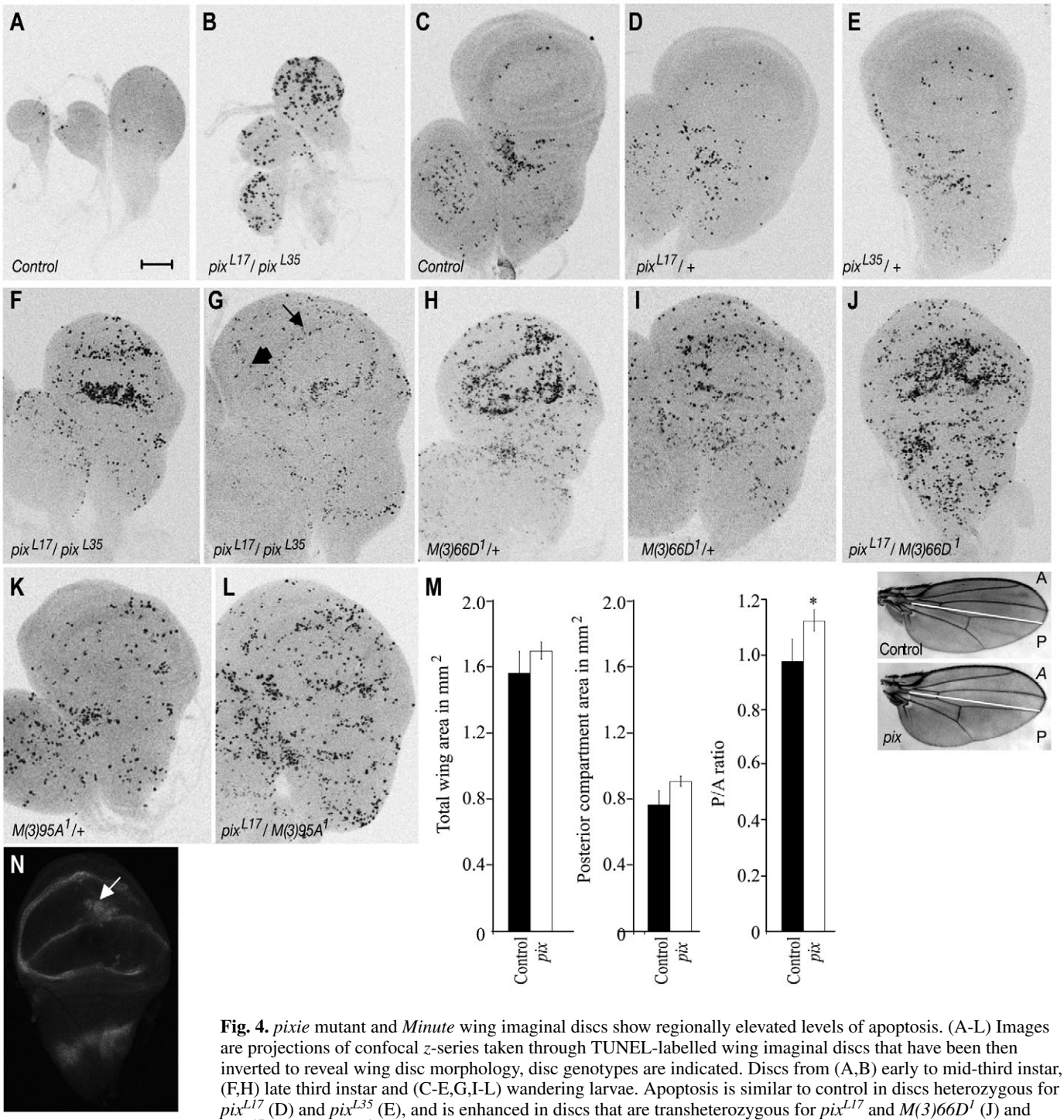

Fig. 4. *pixie* mutant and *Minute* wing imaginal discs show regionally elevated levels of apoptosis. (A-L) Images are projections of confocal *z*-series taken through TUNEL-labelled wing imaginal discs that have been then inverted to reveal wing disc morphology, disc genotypes are indicated. Discs from (A,B) early to mid-third instar, (F,H) late third instar and (C-E,G,I-L) wandering larvae. Apoptosis is similar to control in discs heterozygous for pix^{L17} (D) and pix^{L35} (E), and is enhanced in discs that are transheterozygous for pix^{L17} and $M(3)66D^{1}$ (J) and pix^{L17} and $M(3)95A^{1}$ (L). Thin arrow in G indicates apoptotic nuclei that lie approximately at the DV boundary; thick arrow indicates those that lie at the pouch borders. (M) Bar charts and wing images showing that expressing p35 in the posterior compartment increases area in $pix^{L17/L35}$ wings (*pix*) compared with control (pix^{L17}/+). P/A ratio in *pix* wings is significantly higher than control, $P=3.8\times10^{-10}$. White line in images on the right indicates the AP boundary. (N) Wg protein, detected by immunostaining, is ectopically expressed (arrow) when p35 is expressed in the posterior compartment of *pixie* mutant discs. Scale bar: 50 μm in A-L.

Development

slow phase, *pixie* function is required more in the slowest growing region of the disc and may suggest that Pixie is a target of the constraining signals that slow growth at this stage (see Discussion).

The contribution of cell competition to the *pixie* mutant clone phenotype

The regional differences in the *pixie* growth phenotype may result from regional differences in the intrinsic requirement of the cells for *pixie* function. However, it has been reported that regional differences in mutant clone growth may result from differences in the severity of cell competition across the disc (Simpson, 1979; Moreno et al., 2002; Moreno and Basler, 2004). Cell competition is a process by which the growth of slow-growing clones of mutant cells is further impaired when faster-growing cells surround them (Morata and Ripoll, 1975). Cell competition can be alleviated by making mutant clones in slow-growing *Minute* discs (Morata and Ripoll, 1975).

To study the involvement of cell competition, *pixie* mutant clones were made in the $M(3)66D^{1}$/+ background (henceforth referred to as the *Minute* background), using clone induction windows that span the fast and slow growth phases (Fig. 7A,B). When *pixie* $Minute^{+}$ clones in a *Minute* background are examined at approximately the end of the rapid phase of growth, they are larger than those generated in a non-*Minute* ($Minute^{+}$) background and no longer grow more slowly in the hinge than in the pouch. This is clearly observed by comparing clone size distributions of *pixie* mutant clones in the *Minute* versus $Minute^{+}$ background (compare Fig. 7C with D, and Fig. 7E with F). Thus, *pixie* mutant clones are subject to cell competition; that is, the reduction in mutant clone growth or survival is influenced by the rate of growth of the surrounding cells. These results indicate that the regional differences in *pixie* mutant clone presence during the fast growth phase in normal discs correlates, as a result of cell competition, with the growth rate of the surrounding tissue (see above).

Cell competition has been suggested to be due at least partially to differences in the ability of cells to compete for Dpp (Moreno et al., 2002; Moreno and Basler, 2004). *Minute M(2)C* clones are considered to transduce the Dpp signal inefficiently; thus, these clones ectopically express *brinker* and are eliminated in the wing pouch, a region of high Dpp signalling and low *brinker* expression (Moreno et al., 2002). However, elevated *brinker* expression is not observed in all cases of cell competition (de la Cova et al., 2004). pix^{L17} mutant clones in the wing pouch examined during mid third instar and pre-wandering stages do not express *brinker* (see Fig. S5 in the supplementary material), suggesting that *pixie* mutant clones are not eliminated because of an inability to compete for Dpp.

The *Minute* background enhances the *pixie* mutant clone growth defect during the slow phase

During the slow growth phase, pouch cells grow more slowly than hinge cells; thus, the poor growth of *pixie* mutant clones

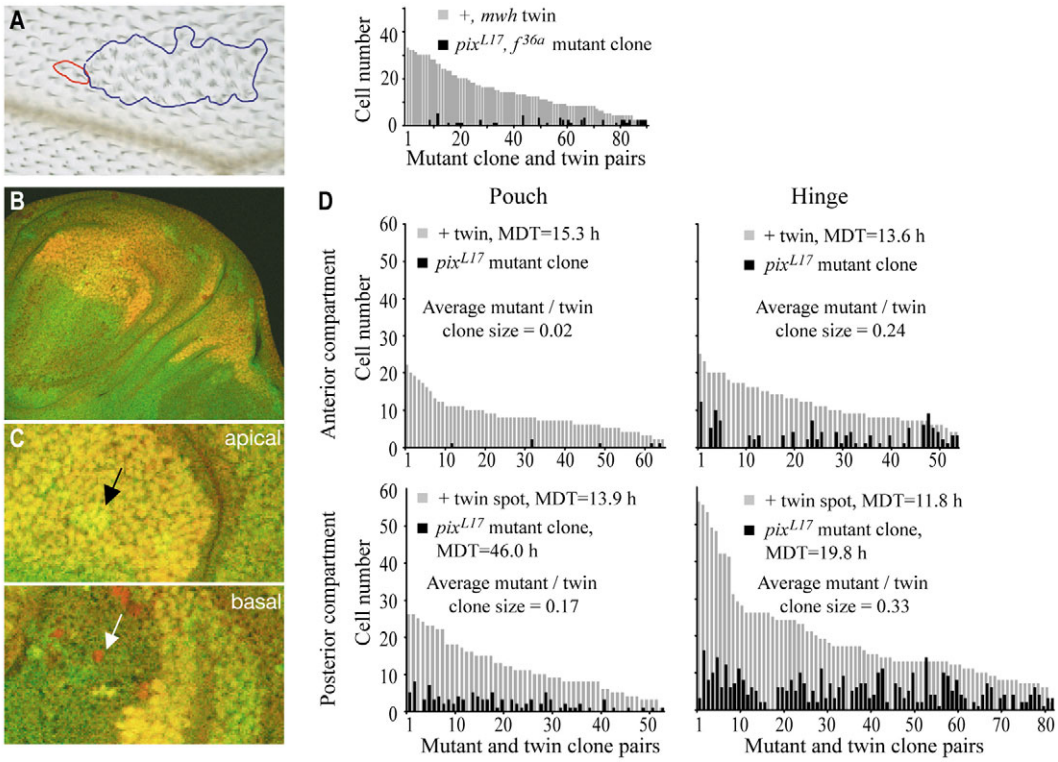

Fig. 5. pix^{L17} causes a reduction in balanced growth and cell survival in wing discs. (A) A pix^{L17}, f^{36a} wing clone (red) induced 27 hours before larval wandering and its accompanying *mwh* twin clone (blue). The presence of the mutant clone does not affect the arrangement of wing hairs in rows, indicating that mutant cell size is not altered. Bar chart on the right shows frequency and cell number of pix^{L17} wing clones (black bars) compared with their twins (grey bars). (B) GFP^{-}, pix^{L17} clones and their $GFP^{+/+}$ twins (examined at wandering stage and induced 46 hours before) in wing discs expressing the capsase inhibitor p35 in the posterior compartment (labelled using anti-En, red or orange when merged with GFP). (C) Apical (above) and basal (below) confocal sections through the same disc showing that nuclei of surviving pix^{L17} clones (white arrow) in the posterior pouch are more basal than their accompanying twins (black arrow). (D) Bar charts representing the number of cells in pix^{L17}clones (black), and their twins (grey) in anterior clones (above) and in posterior p35-expressing clones (below); pouch clones are on left and hinge clones on right. TUNEL labelling confirmed that p35 expression blocked apoptosis (data not shown). Although posterior mutant clones are larger, the average mutant/twin clone size in the posterior compartment is still significantly less in the pouch (0.17) than the hinge (0.33), $P<0.0001$.

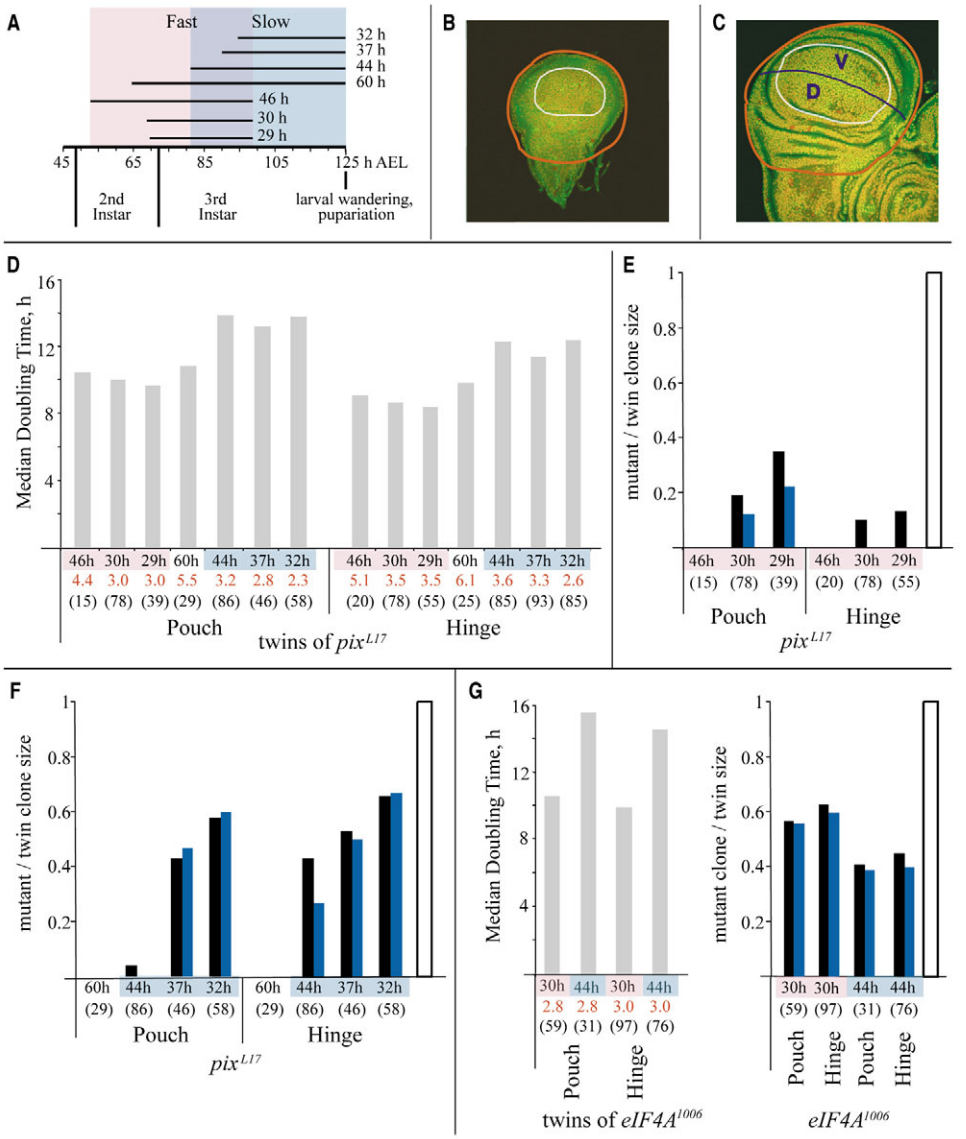

Fig. 6. Spatial and temporal dynamics of the effect of *pix*^{L17} and *eIF4A*^{1006} on wing disc clonal growth. (A) A schematic showing the different clone induction windows used. Larval stage and developmental time in hours AEL is shown below. Black bars above indicate start and end of each clone induction window; duration is shown in hours (h) on right of each bar. Windows representing the 'fast' phase end at mid-third instar (pink box); those representing the 'slow' phase end at larval wandering and are within the blue box. The 60-hour window spans both phases. The boxes overlap; however, there is a time lag between the time of clone induction and clone generation, and MDT analysis (D) reveals that the actual overlap in the life of the clones is likely to be minimal (see Materials and methods). (B,C) Images of *pix*^{L17}*/GFP* heterozygous discs with clones at mid-third instar (B) and a wandering third instar (C). The wing pouch, recognized as the unfolded epithelium at the centre of the disc, is marked by a white line; a blue line marks the DV boundary. The region regarded as hinge in our experiments surrounds the pouch and is within the red line. It includes regions that contribute to the ventral thorax, and, in early discs, the distal notum. (D-G) Bar charts in grey show the wild-type twin (GFP$^{+/+}$) MDTs. Black and blue bar charts show mutant/twin clone size as average (black bars) and median (dark blue bars) with unfilled bars on right of each chart depicting a ratio of 1, which would indicate no effect on growth, for comparison. When clones are frequently absent, the median clone/twin size is 0, or much smaller than the average clone/twin size. As shown in A, pink and blue boxes mark clones examined at mid third instar or at wandering, respectively; the region examined (pouch or hinge) and genotype of clones (*pix*^{L17} and *eIF4A*^{1006}) is indicated. *x*-axis shows clone induction window lengths (h), the median number of divisions within the twins (red) and the number of twins analyzed (n). Fig. S4 in the supplementary material shows raw clone and twin cell number data for the above experiments.

in the pouch is unlikely to be due to stronger cell competition there. Indeed, our analysis reveals that the representation of *pixie* mutant clones at this stage is not improved in a *Minute* background (compare Fig. 7G with H and Fig. 7I with J). In the hinge, it is difficult to estimate *pixie* mutant clone growth in the *Minute* background because of clone fragmentation (see Materials and methods). However, a growth advantage is not visible. In the pouch, *pixie* mutant clones actually grow more poorly in a *Minute* background than those made in the *Minute*$^{+}$ background. It is clear that differences in *pixie* mutant clone growth between the pouch and hinge are maintained, and even exaggerated, in the *Minute* background. An impairment of clone growth in a *Minute* background has not been reported for other mutant clones. It is likely that during the slow phase, wing pouch cells require sufficient levels of Pixie and Rp function in neighbouring cells for normal growth. *Minute*$^{-/-}$ clones are rapidly eliminated because of their very low level of Rp function. We have noted that in the above *Minute* environment, *Minute*$^{-/-}$ clones are more rapidly eliminated during the slow phase than during the fast phase (Fig. 7), suggesting that the *Minute* environment during the slow phase constrains growth/cell survival.

To ensure that the *Minute* background used in these experiments effectively reduces cell competition during the slow growth phase, the growth of wild-type (M^{+}) clones in the same *Minute* background was examined. These M^{+} clones do have a growth advantage and are larger than those generated in a *Minute*$^{+}$ background, as previously described for other *Minutes* (Simpson and Morata, 1981) (compare Fig. 7K with L). Thus, this *Minute* background reduces cell competition. Intriguingly, although M^{+} clones have a growth advantage in this *Minute* background, pouch clones still grow more slowly

Development

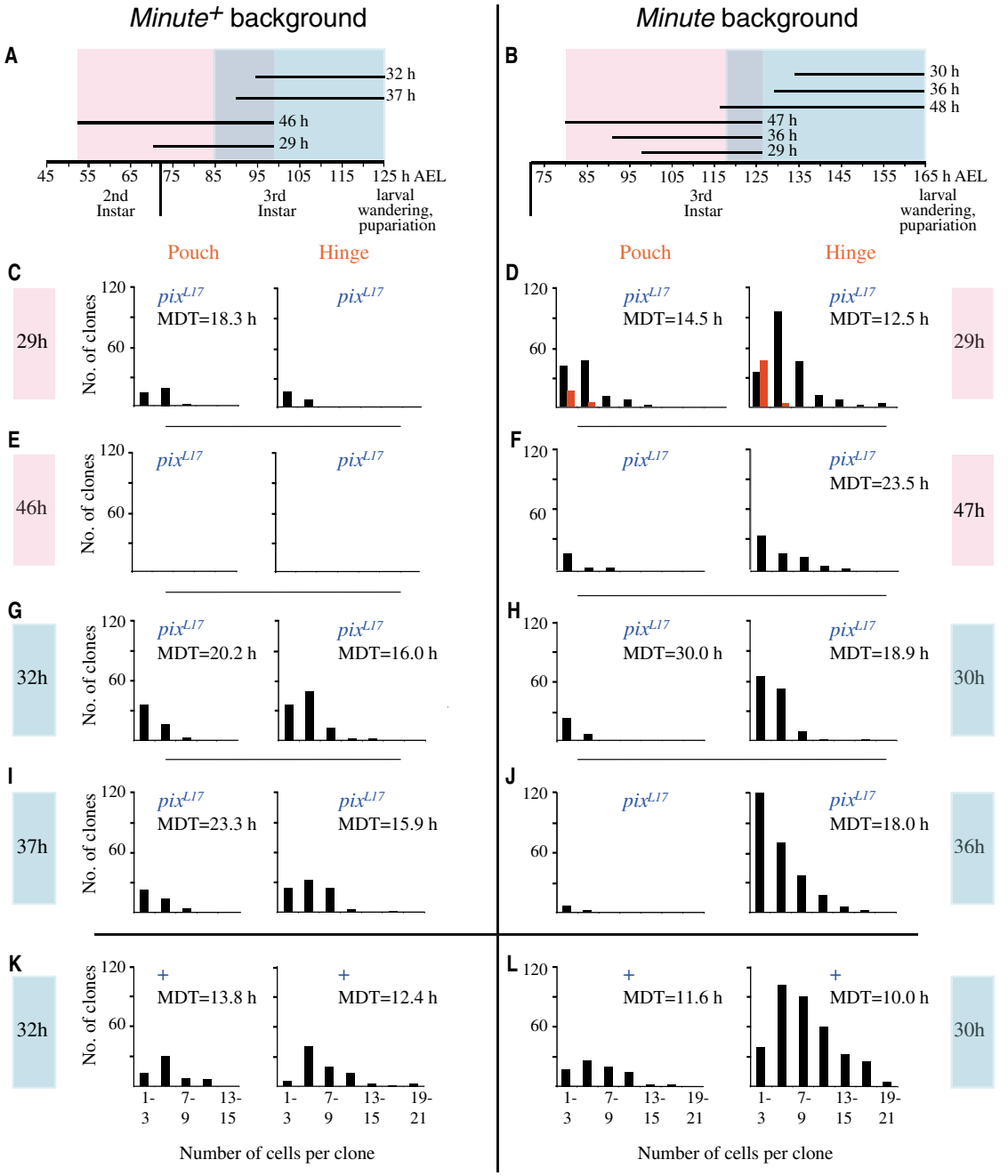

Fig. 7. A *Minute* background has different effects on the growth of *pix*^{L17} clones during fast and slow growth. (A,B) Schematics showing the stages of development and clone induction windows used. Blue boxes represent discs examined at larval wandering and pink boxes discs examined at approximately mid-third instar. (C-L) Bar charts depicting clone size distributions of *pix*^{L17}, *Minute*$^{+}$ clones (C-J) and wild-type clones (K-L) as control. When *Minute*$^{+/+}$ (*Minute*$^{+}$) clones are generated in a *Minute*$^{+/-}$ (*Minute*) background, the *Minute*$^{-/-}$ twins survive poorly and cannot be used to assess background tissue growth. Thus, the size distribution of clones in a *Minute* background (right) is compared with the size of *pix*^{L17} or wild-type clones generated in a normal, *Minute*$^{+}$ background (left), using comparable clone induction window lengths and stages of development. *Minute*$^{-/-}$ twins survive better during the fast phase and are shown as red bars in D. In the other experiments, these twins are rarely found. For example, among the clones depicted in H, four in the hinge were accompanied by twins. They are even more rare in the experiments depicted in F and L and are not seen in J. Twin clones in the *Minute*$^{+}$ background are not depicted because this data is shown in Fig. 6. *x*-axes show size categories of clone cell number and *y*-axes show number of clones in each category. When sufficient numbers of clones are present, MDT is indicated. Difference in clone growth between pouch and hinge in D,F and L is significant, $P<0.005$ in D and F; $P<0.000001$ in L.

than hinge clones (Fig. 7L). Furthermore, during the fast phase, although the growth of *pixie* mutant clones is enhanced in a *Minute* compared with *Minute*$^{+}$ background, these clones also grow more slowly in the pouch than the hinge (Fig. 7D,F). Thus, growth constraints exist in the pouch during most of the third instar. Put together our data suggests that although a *Minute*

Development

background reduces cell competition, it reveals the presence of growth constraints that exist in wing discs. During the slow phase, these constraints are more severe or act more severely on slow growing cells that are mutant for *pixie* or *Rp* function. As the pattern of these constraints resemble the regional and temporal differences in wild-type clone growth, they are likely to reflect the constraints that normally exist in disc growth.

Discussion

To summarize, we have characterized the role of Pixie, a newly identified *Drosophila* ABC-E protein, in growth control. We have shown that in S2 cells, Pixie is required for normal translation. During wing disc development, its requirement in growth and cell survival varies spatially and temporally. Our clonal analysis suggests that this variation in requirement correlates with growth rate of the surrounding tissue, albeit in an unexpected manner. During the fast growth phase, Pixie is required more in a faster growing region of the disc; during the slow phase, Pixie is required more in a slow growing region.

We have found that reduced Rp and Pixie function, but not EIF4A function, results in regional differences in growth and cell survival. The molecular basis for these differences is not immediately clear and suggests that reducing the function of different components of the translation machinery can have different effects on disc growth and cell survival. Our results imply that the regional differences in growth rates across the wing disc are not accompanied by regional differences in levels of translation that are large enough to result in detectable differences in the requirement for *eIF4A* (Johnston and Sanders, 2003; Garcio-Bellido and Merriam, 1971) (data shown here). By contrast, the requirement for *pixie* and *rp* function does seem to reflect regional differences in other properties that reflect the non-homogenous nature of wing disc cells. It is intriguing that reducing *rp* or *pixie* function does not result in randomly distributed clusters of dying cells throughout the wing disc throughout development, instead these clusters are elevated in the wing pouch towards the end of development. However, this non-homogenous nature of wing disc cells is not easily explained by what is known about the activities of signalling pathways that regionally regulate cell survival and proliferation in the wing disc. For example, Wg and Dpp signalling are required for cell survival and balanced growth in the wing pouch (Neumann and Cohen, 1996; Giraldez and Cohen, 2003; Johnston and Sanders, 2003; Martin-Castellanos and Edgar, 2002; Moreno et al., 2002). A temporal analysis of the requirement for Wg signalling revealed that Wg is required more strongly in the wing pouch for cell survival during the fast growth phase (Johnston and Sanders, 2003). This contrasts with the pattern of cell death observed in *pixie* mutant and *Minute* discs. Furthermore, clonal analysis suggests that during the fast growth phase, *pixie* is required more in the hinge than in the wing pouch. Johnston and Sanders also suggest that Wg signalling constrains balanced growth in the wing pouch during the late stages of disc growth. This observation is compatible with the poor growth of *pixie* mutant clones in the wing pouch during slow phase (see below). However, it is not compatible with a potential role for Wg in compensation of *pixie* mutant cell death (Huh et al., 2004; Perez-Garijo et al., 2004).

Similar to the *eIF4A* mutant clones, insulin-signalling mutants have not been reported to show regional differences in their effect on wing disc clone growth (S.J.L., unpublished). Besides *Minute* and *pixie* mutant clones, clones that express lower levels of Myc also show regional differences in their growth in wing discs (Simpson, 1979; Moreno et al., 2002; Moreno and Basler, 2004). Myc has recently been shown to regulate levels of rRNA and also has the potential to regulate levels of ribosomal proteins (Grewal et al., 2005). Thus far, these regional effects in clone growth of Myc-underexpressing and *Minute* clones have been attributed to differences in the severity of cell competition (Moreno et al., 2002; Moreno and Basler, 2004). Our findings however, raise the possibility that some of these regional effects are due to sensitivity to growth constraints. During the slow growth phase, the strong *pixie* clone phenotype in the pouch is better explained by an increased sensitivity to growth-constraining signals, rather than competition from faster-growing neighbouring cells.

A model to explain how Pixie might respond to growth constraining signals

A possible explanation for the dynamic spatial requirement for *pixie* is that *pixie* responds to growth promoters that are limiting for growth and also show dynamic spatial expression. However, it is hard to explain why levels of these growth promoters would be limiting in the early hinge and late pouch (where the *pixie* clone phenotype is stronger), and not the early pouch and late hinge (where the *pixie* clone phenotype is weaker). Thus, it is unlikely that the varying effects on *pixie* mutant clone growth can be explained purely on the basis of the differential activity of growth promoters. In addition, we observe that reducing cell competition in *Minutes* does not remove the regional differences in growth rate of *Minute*$^{+}$ clones with a growth advantage – pouch clones still grow more slowly than hinge clones. Our data are more easily explained by a model in which growth results from a balance between the activities of growth promoters and inhibitors. The inhibitors antagonize the activity of the promoters and are at higher levels in the pouch; *pixie* mutant cells show increased sensitivity to the growth inhibitors. Thus, we propose that during the fast phase, levels of growth inhibitors are low and growth promoters high, and *pixie* is required more where growth is faster. As inhibitor levels rise during the slow phase and promoter activity drops, *pixie* is now required more where inhibitor levels are higher. *pixie* function may be the direct or indirect target of inhibitor activity. Alternatively, *pixie* function may counteract the activity of the inhibitors.

The model proposed above is based partly on a hypothetical, mathematically simulated model described by Nijhout to explain how disc size is sensed and growth stopped (Fig. 8) (Nijhout, 2003). This model proposes that inhibitor levels are low during the exponential phase of growth, but rise as disc growth slows and remain high during the slow growth phase. Thus, Nijhout's model proposes differential gene activity (differences in inhibitor levels) between the fast and slow growth phases. Computer simulations using Nijhout's model show that increases in cell number correlate with changes in activator and inhibitor concentrations over time, and resemble the observed growth curve of imaginal discs. However, our model also requires that the inhibitors are at higher levels in the pouch and thus it is an adaptation of Nijhout's model (Fig. 8). The 'gradient of responsiveness' model, which also

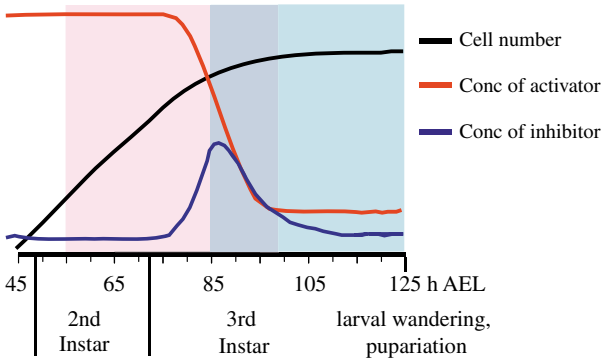

Fig. 8. Model depicting changing levels of growth activators and inhibitors synthesized by disc cells in relation to increases in cell number. This model is a variation of a model proposed by Nijhout to explain how rising levels of growth inhibitors may determine disc size (Nijhout, 2003). In Nijhout's model, imaginal disc cells produce growth activators and inhibitors, and the inhibitors sequester or inactivate the activators. The level of each factor depends on the number of cells at the time and the influence of the inhibitor over the activator. At first activator levels are high, inhibitor levels low and disc growth is approximately exponential. When inhibitor levels become sufficiently high, growth begins to slow. Nijhout's model proposes that inhibitor activity remains high throughout slow growth. Accordingly, if *pixie* mutant cells were sensitive to the presence of inhibitor, then *pixie* mutant clone growth would be expected to worsen towards the end of larval life and during metamorphosis as growth slows. Instead, *pixie* mutant clone growth (survival) improves at the end of larval life (see text and Fig. 6E,F), and the intensity of cell death in *pixie* mutant and *Minute* discs decreases shortly before pupation (Fig. 4). Thus, we propose that the presence of activator is necessary for inhibitor synthesis. When inhibitor levels reach a threshold, this triggers the slowing down of growth and inactivation of the activator, which in turn leads to downregulation of inhibitor synthesis. Thus the *pixie* mutant clone phenotype is strong at the beginning of the slow phase, when inhibitor levels are high, but weak at the end of larval life when inhibitor levels are low, and growth is slow. The graphs presented here potentially apply to both the hinge and the pouch, with higher levels of inhibitors being found in the pouch than the hinge.

proposes a role for inhibitors in the determination of size, suggests that inhibitors may exist at higher levels in the pouch to counteract the effects of morphogens that are expressed at higher levels there (Serrano and O'Farrell, 1997).

The model presented in Fig. 8 explains broadly the observations made in this paper. However, the hypothesized inhibitors need to be identified. Nijhout's model presumes that all disc cells synthesize growth promoters and inhibitors (an insulin-like peptide is synthesized by disc cells) (Brogiolo et al., 2001). Our adaptation to this model suggests that the inhibitors are synthesized by all disc cells but at higher levels in the disc pouch. Nitric oxide (NO) has been shown to inhibit growth during the late third instar and high levels of NO activity are detected in the wing pouch in late third instar discs (Kuzin et al., 1996). However, the ability of NO to inhibit growth and cell division is only evident shortly before pupation. The pattern of cell death in *pixie* mutant discs together with the clonal analysis suggests that the proposed sensitivity to growth inhibitor might decrease shortly before pupation (see Fig. 8). Furthermore, we have found that injecting nitric oxide synthase inhibitors into larvae does not reduce cell death in late *pixie* mutant discs, and in fact occasionally exacerbates it (data not shown). Thus, *pixie* mutant cells are not dying because of an increased sensitivity to NO. Wg signalling has been proposed to constrain growth in the wing pouch during late larval life (Johnston and Sanders, 2003). However, as discussed above, any interaction between Wg signalling and the *pixie* mutant phenotype is likely to be complex.

A mild reduction in Pixie function results in an impairment of balanced growth and cell survival that varies regionally and temporally in wing discs. This impairment shows the classical characteristics of compensation known to occur for example in wing discs subjected to X-irradiation (Haynie and Bryant, 1977). Despite intensive cell death, close to normal final disc size is achieved, without disturbing differentiation and pattern. However, the observed ability of *pixie* mutant and *Minute* cells to compensate for defects in survival and growth that occur earlier in development is interesting and emphasises the intrinsic ability of these mutant cells to grow and survive. The varying patterns of cell death with time can be seen as a reflection of the different growth environments that these cells are subjected to as development progresses. These mutant cells succumb to the changing environment but do not fully interfere with the ability of the system to correct the defects that arise due to cell death or even perhaps extra cell proliferation. However, it is clear that this ability of the system to correct itself is compromised to the extent that proportion is not always maintained and mild overgrowth can occur (see Marygold et al., 2005; Coelho et al., 2005). Studying the ability of mutant tissues to respond to growth constraints in vivo should advance our understanding of how the slowing down of growth is triggered.

We are very grateful to Robin Wharton for providing additional *pixie* alleles, and to Mireille Galloni, Bruce Edgar, Antonio Garcia-Bellido and Steve Kerridge for additional reagents. We also thank Nicolas Tapon, Helen McNeill, Pascal Meier, David Ish-Horowicz and Buzz Baum for much advice on the preparation of this manuscript. We thank the London Research Institute Electron Microsocopy Unit, Light Microscopy Unit, FACS laboratory and fly facility for their help. C.M.A.C. gratefully acknowledges K. VijayRagahavan and Veronica Rodrigues and members of their laboratories at the NCBS for their help and generous support during a part of this work. This work was supported by the Medical Research Council, The Ludwig Institute for Cancer Research and Cancer Research UK.

Supplementary material

Supplementary material for this article is available at
http://dev.biologists.org/cgi/content/full/132/24/5411/DC1

References

Bisbal, C., Silhol, M., Laubenthal, H., Kaluza, T., Carnac, G., Milligan, L., Le Roy, F. and Salehzada, T. (2000). The 2′-5′ oligoadenylate/RNase L/RNase L inhibitor pathway regulates both MyoD mRNA stability and muscle cell differentiation. *Mol. Cell. Biol.* **20**, 4959-4969.

Brogiolo, W., Stocker, H., Ikeya, T., Rintelen, F., Fernandez, R. and Hafen, E. (2001). An evolutionarily conserved function of the Drosophila insulin receptor and insulin-like peptides in growth control. *Curr. Biol.* **11**, 213-221.

Brower, D. L. (1986). Engrailed gene expression in Drosophila imaginal discs. *EMBO J.* **5**, 2649-2656.

Bryant, P. J. and Simpson, P. (1984). Intrinsic and extrinsic control of growth in developing organs. *Q. Rev. Biol.* **59**, 387-415.

Bryant, P. J. and Levinson, P. (1985). Intrinsic growth control in the imaginal

primordia of Drosophila, and the autonomous action of a lethal mutation causing overgrowth. *Dev. Biol.* **107**, 355-363.
Clemens, J. C., Worby, C. A., Simonson-Leff, N., Muda, M., Maehama, T., Hemmings, B. A. and Dixon, J. E. (2000). Use of double-stranded RNA interference in Drosophila cell lines to dissect signal transduction pathways. *Proc. Natl. Acad. Sci. USA* **97**, 6499-6503.
Coelho, C. M. and Leevers, S. J. (2000). Do growth and cell division rates determine cell size in multicellular organisms? *J. Cell Sci.* **113**, 2927-2934.
Coelho, C. M., Kolevski, B., Walker, C. D., Lavagi, I., Shaw, T., Ebert, A., Leevers, S. J. and Marygold, S. J. (2005). A genetic screen for dominant modifiers of a small-wing phenotype identifies proteins involved in splicing and translation in Drosophila melanogaster. *Genetics* **171**, 597-614.
Cohen, S. (1993). Imaginal disc development. In *The Development of* Drosophila melanogaster (ed. M. Bate and A. M. Arias), pp. 747-842. New York: Cold Spring Harbor Laboratory Press.
Dahanukar, A., Walker, J. K. and Wharton, R. P. (1999). Smaug, a novel RNA-binding protein that operates a translational switch in Drosophila. *Mol. Cell* **4**, 209-218.
Datar, S. A., Jacobs, H. W., de la Cruz, A. F., Lehner, C. F. and Edgar, B. A. (2000). The Drosophila Cyclin D-Cdk4 complex promotes cellular growth. *EMBO J.* **19**, 4543-4554.
Day, S. J. and Lawrence, P. A. (2000). Measuring dimensions: the regulation of size and shape. *Development* **127**, 2977-2987.
de la Cova, C., Abril, M., Bellosta, P., Gallant, P. and Johnston, L. A. (2004). Drosophila myc regulates organ size by inducing cell competition. *Cell* **117**, 107-116.
Dean, M. and Allikmets, R. (2001). Complete characterization of the human ABC gene family. *J. Bioenerg. Biomembr.* **33**, 475-479.
Dong, J., Lai, R., Nielsen, K., Fekete, C. A., Qiu, H. and Hinnebusch, A. G. (2004). The essential ATP-binding cassette protein RLI1 functions in translation by promoting preinitiation complex assembly. *J. Biol. Chem.* **279**, 42157-42168.
Dooher, J. E. and Lingappa, J. R. (2004). Conservation of a stepwise, energy-sensitive pathway involving HP68 for assembly of primate lentivirus capsids in cells. *J. Virol.* **78**, 1645-1656.
Farmer, M. A. and German, R. Z. (2004). Sexual dimorphism in the craniofacial growth of the guinea pig (Cavia porcellus). *J. Morph.* **259**, 172-181.
Galloni, M. and Edgar, B. A. (1999). Cell-autonomous and non-autonomous growth-defective mutants of Drosophila melanogaster. *Development* **126**, 2365-2375.
Garcia-Bellido, A. and Merriam, J. R. (1971). Parameters of the wing imaginal disc development in Drosophila melanogaster. *Dev. Biol.* **26**, 61-87.
Giraldez, A. J. and Cohen, S. M. (2003). Wingless and Notch signaling provide cell survival cues and control cell proliferation during wing development. *Development* **130**, 6533-6543.
Gonzalez-Gaitan, M., Capdevilla, M. P. and Garcia-Bellido, A. (1994). Cell proliferation patterns in the wing imaginal disc of Drosophila. *Mech. Dev.* **40**, 183-200.
Grewal, S. S., Li, L., Orian, A., Eisenman, R. N. and Edgar, B. A. (2005). Myc-dependent regulation of ribosomal RNA synthesis during Drosophila development. *Nat. Cell Biol.* **7**, 295-302.
Hay, B. A., Wolff, T. and Rubin, G. M. (1994). Expression of baculovirus P35 prevents cell death in Drosophila. *Development* **120**, 2121-2129.
Haynie, J. L. and Bryant, P. J. (1977). The effects of X-rays on the proliferation dynamics of cells in the imaginal disc of Drosophila melanogaster. *Roux's Arch.* **183**, 85-100.
Huh, J. R., Guo, M. and Hay, B. A. (2004). Compensatory proliferation induced by cell death in the Drosophila wing disc requires activity of the apical cell death Caspase Dronc in a nonapoptotic role. *Curr. Biol.* **14**, 1262-1266.
Johnston, L. A. and Edgar, B. A. (1998). Wingless and Notch regulate cell-cycle arrest in the developing Drosophila wing. *Nature* **394**, 82-84.
Johnston, L. A. and Sanders, A. L. (2003). Wingless promotes cell survival but constrains growth during Drosophila wing development. *Nat. Cell Biol.* **5**, 827-833.
Kerr, I. D. (2004). Sequence analysis of twin ATP binding cassette proteins involved in translational control, antibiotic resistance, and ribonuclease L inhibition. *Biochem. Biophys. Res. Commun.* **315**, 166-173.
Kispal, G., Sipos, K., Lange, H., Fekete, Z., Bedekovics, T., Janaky, T., Bassler, J., Aguilar Netz, D. J., Balk, J., Rotte, C. and Lill, R. (2005). Biogenesis of cytosolic ribosomes requires the essential iron-sulphur protein Rli1p and mitochondria. *EMBO J.* **24**, 589-598.
Kuzin, B., Roberts, I., Peunova, N. and Enikolopov, G. (1996). Nitric oxide regulates cell proliferation during Drosophila development. *Cell* **87**, 639-649.
Lambertsson, A. (1998). The Minute genes in Drosophila and their molecular functions. *Adv. Genet.* **38**, 69-134.
Leevers, S. J. and Hafen, E. (2004). Growth regulation by insulin and TOR signalling. In *Cell Growth, Control of Cell Size* (ed. M. N. Hall, M. Raff and G. Thomas), pp. 167-192. New York: Cold Spring Harbor Laboratory Press.
Leevers, S. J., Weinkove, D., MacDougall, L. K., Hafen, E. and Waterfield, M. D. (1996). The Drosophila phosphoinositide 3-kinase Dp110 promotes cell growth. *EMBO J.* **15**, 6584-6594.
Lizcano, J. M., Alrubaie, S., Kieloch, A., Deak, M., Leevers, S. J. and Alessi, D. R. (2003). Insulin-induced Drosophila S6 kinase activation requires phosphoinositide 3-kinase and protein kinase B. *Biochem. J.* **374**, 297-306.
Martin-Castellanos, C. and Edgar, B. A. (2002). A characterization of the effects of Dpp signaling on cell growth and proliferation in the Drosophila wing. *Development* **129**, 1003-1013.
Marygold, S. J., Coelho, C. M. and Leevers, S. J. (2005). Genetic analysis of RpL38 and RpL5, two Minute genes located in the centric heterochromatin of chromosome 2 of Drosophila melanogaster. *Genetics* **169**, 683-695.
Milan, M., Campuzano, S. and Garcia-Bellido, A. (1996). Cell cycling and patterned cell proliferation in the wing primordium of Drosophila. *Proc. Natl. Acad. Sci. USA* **93**, 640-645.
Milan, M., Campuzano, S. and Garcia-Bellido, A. (1997). Developmental parameters of cell death in the wing disc of Drosophila. *Proc. Natl. Acad Sci. USA* **94**, 5691-5696.
Morata, G. and Ripoll, P. (1975). Minutes: mutants of drosophila autonomously affecting cell division rate. *Dev. Biol.* **42**, 211-221.
Moreno, E. and Basler, K. (2004). dMyc transforms cells into super-competitors. *Cell* **117**, 117-129.
Moreno, E., Basler, K. and Morata, G. (2002). Cells compete for decapentaplegic survival factor to prevent apoptosis in Drosophila wing development. *Nature* **416**, 755-759.
Neufeld, T. P., de la Cruz, A. F., Johnston, L. A. and Edgar, B. A. (1998). Coordination of growth and cell division in the Drosophila wing. *Cell* **93**, 1183-1193.
Neumann, C. J. and Cohen, S. M. (1996). Distinct mitogenic and cell fate specification functions of wingless in different regions of the wing. *Development* **122**, 1781-1789.
Nijhout, H. F. (2003). The control of body size in insects. *Dev. Biol.* **261**, 1-9.
Perez-Garijo, A., Martin, F. A. and Morata, G. (2004). Caspase inhibition during apoptosis causes abnormal signalling and developmental aberrations in Drosophila. *Development* **131**, 5591-5598.
Postlethwait, J. H. (1978). Clonal analysis of Drososphila cuticular patterns, In *The Genetics and Biology of Drosophila* (ed. M. Ashburner and T. R. F. Wright), Vol. 2c, pp. 359-441. New York: Academic Press.
Prober, D. A. and Edgar, B. A. (2000). Ras1 promotes cellular growth in the Drosophila wing. *Cell* **100**, 435-446.
Reichling, T. and German, R. Z. (2000). Protein malnutrition in Rattus norvegicus increases the duration of growth of muscles, bones and visceral organs allowing malnourished individuals to reach similar final sizes as controls. *J. Nutrition* **130**, 2326-2332.
Serrano, N. and O'Farrell, P. H. (1997). Limb morphogenesis: connections between patterning and growth. *Curr. Biol.* **7**, R186-R195.
Simpson, P. (1979). Parameters of cell competition in the compartments of the wing disc of Drosophila. *Dev. Biol.* **69**, 182-193.
Simpson, P. and Morata, G. (1981). Differential mitotic rates and patterns of growth in compartments in the Drosophila wing. *Dev. Biol.* **85**, 299-308.
Stewart, S. A. and German, R. Z. (1999). Sexual dimorphism and ontogenetic allometry of soft tisuues in Rattus norvegicus. *J. Morphol.* **242**, 57-66.
Tyzack, J. K., Wang, X., Belsham, G. J. and Proud, C. G. (2000). ABC50 interacts with eukaryotic initiation factor 2 and associates with the ribosome in an ATP-dependent manner. *J. Biol. Chem.* **275**, 34131-34139.
White, K., Lisi, S., Kurada, P., Franc, N. and Bangs, P. (2001). Methods for studying apoptosis and phagocytosis of apoptotic cells in Drosophila tissues and cell lines. *Methods Cell Biol.* **66**, 321-338.
Xu, T. and Rubin, G. M. (1993). Analysis of genetic mosaics in developing and adult Drosophila tissues. *Development* **117**, 1223-1237.
Yarunin, A., Panse, V. G., Petfalski, E., Dez, C., Tollervey, D. and Hurt, E. C. (2005). Functional link between ribosome formation and biogenesis of iron-sulfur proteins. *EMBO J.* **24**, 580-588.
Zimmerman, C., Klein, K. C., Kiser, P. K., Singh, A. R., Firestein, B. L., Riba, S. C. and Lingappa, J. R. (2002). Identification of a host protein essential for assembly of immature HIV-1 capsids. *Nature* **415**, 88-92.